

広帯域MT法による地殻内流体の3次元分布解明 3D imaging of geofluid by wideband magnetotellurics

小川 康雄^{1*}; 市來 雅啓²; 神田 径¹
OGAWA, Yasuo^{1*}; ICHIKI, Masahiro²; KANDA, Wataru¹

¹ 東京工業大学火山流体研究センター, ² 東北大学大学院理学研究科

¹ Volcanic Fluid Research Center, Tokyo Institute of Technology, ² Graduate School of Science, Tohoku University

Magnetotelluric measurements have been conducted over the five years in the central part of NE Japan arc surrounding the Naruko Volcano with approximately 3km grid. Over 200 sites were used for modeling the crustal resistivity structure in detail. Full impedance tensors for 8 periods were used for inversion. To alluviate the computational load, first four short periods were used to image upper crustal features and the resultant model was used for a prior model for another set of inversions with longer 4 periods.

The obtained model show the crustal conductor underneath the Mukaimachi caldera and Sanzugawa caldera. Seismic tomography shows low S-wave velocity for both, however, the resistivity image show clear low resistivity for Mukaimachi Caldera, but not for Sanzugawa Caldera. This difference may be due to the salinity of the fluids underlying the volcanic regions.

キーワード: 地殻流体, マグネトテルリクス, 比抵抗, 3次元構造
Keywords: geofluid, magnetotellurics, resistivity, 3d

東北地方上部マントル沈み込み帯の3次元電気伝導度構造 Three dimensional electrical conductivity model in the subduction zone beneath north-eastern Japan

市來 雅啓^{1*}; 小川 康雄²; 海田 俊輝¹; 出町 知嗣¹; 平原 聡¹; 本蔵 義守²; 市原 寛³; 神田 径²; 河野 俊夫¹; 小山 崇夫⁴; 松島 政貴⁵; 中山 貴史¹; 鈴木 秀市¹; 藤 浩明⁶; 上嶋 誠⁴
ICHIKI, Masahiro^{1*}; OGAWA, Yasuo²; KAIDA, Toshiki¹; DEMACHI, Tomotsugu¹; HIRAHARA, Satoshi¹; HONKURA, Yoshimori²; ICHIHARA, Hiroshi³; KANDA, Wataru²; KONO, Toshio¹; KOYAMA, Takao⁴; MATSUSHIMA, Masaki⁵; NAKAYAMA, Takashi¹; SUZUKI, Shu'ichi¹; TOH, Hiroaki⁶; UYESHIMA, Makoto⁴

¹ 東北大学大学院理学研究科, ² 東京工業大学火山流体研究センター, ³ 海洋研究開発機構地球内部ダイナミクス領域, ⁴ 東京大学地震研究所, ⁵ 東京工業大学大学院理工学研究科, ⁶ 京都大学大学院理学研究科
¹Grad. School of Sci., Tohoku University, ²VFRC, Tokyo Institute of Technology, ³IFREE, JAMSTEC, ⁴ERI, The University of Tokyo, ⁵Grad. School of Sci. & Eng., Tokyo Tech, ⁶Grad. School of Sci., Kyoto University

Our final goal is to infer a geofluid map (GFM) from both of the seismological (seismic velocity, V_p/V_s , Q etc.) and electrical conductivity structures in the wedge mantle of subduction zone beneath northeastern Japan. While plenty of high-resolution three dimensional (3-D) seismic tomographic images has been revealed there, none of 3-D electrical conductivity distribution model, of which the resolution is comparative to those of seismic tomography, has been proposed in terms of wedge mantle in subduction zones. Here, we show a high-resolution 3-D electrical conductivity distribution model in the wedge mantle beneath northeastern Japan used as input of GFM.

We carried out long-period MT observation using the state-of-the-art equipments, LEMI-417 and NIMS. The total 72 site observation has been completed. To remove tilt changes, baseline steps and drifts of fluxgate magnetometers, we first subtracted magnetic field variations to which a median filter was applied, from raw data. The horizontal coordinate of magnetic field data in each site was rotated before the response calculation such that the declination of the averaged horizontal component should be consistent with the 2010 absolute geomagnetic observation map provided by Geospatial Information Authority of Japan. We used the BIRRP processing code (Chave and Thomson, 2004) to estimate MT responses and have successfully retrieved them up to 61440 seconds in period.

The MT impedance responses were inverted into 3-D electrical conductivity model using WSINV3D (Siripunvaraporn et al, 2005), the data-space Occam inversion method. The all input data error floor was assigned to be 10 percent. We investigated the optimal reference model with trial and errors. The test model was (1) uniform models, (2) layered models and (3) layered models with subducting slab models. The best RMS in each reference model was (1) 2.81, (2) 2.71 and (3) 2.48, respectively. Hence, we adopted the reference model of the layered model with subducting slab.

The conductivity profiles normal to the trench axis in higher latitude than N 39 degrees delineate conductive region on the subducting slab, and the conductive region is raised just beneath the central range of northeastern Japan (Ou-backbone range). This electrical image is well consistent with that obtained by the seismic tomographic model. On the other hand, a profile in lower latitude than N 39 degrees reveals that the conductive region is overturned towards backarc. The top of the overturned conductive body coincides with Gassan Volcano location, one of the outstanding backarc volcanism. However, Chokai Volcano, another distinctive backarc volcanism has no subsurface conductive root originated from deep upper mantle. The overturned mantle convection image is not found in the seismic tomographic image.

S-wave attenuation on the western side of Nankai subduction zone: implications for geofluid distribution and dynamics

S-wave attenuation on the western side of Nankai subduction zone: implications for geofluid distribution and dynamics

高橋 努^{1*}; 尾鼻 浩一郎¹; 山本 揚二郎¹; 仲西 理子¹; 小平 秀一¹; 金田 義行¹
TAKAHASHI, Tsutomu^{1*}; OBANA, Koichiro¹; YAMAMOTO, Yojiro¹; NAKANISHI, Ayako¹; KODAIRA, Shuichi¹; KANEDA, Yoshiyuki¹

¹ (独) 海洋研究開発機構
¹JAMSTEC

One major cause of seismic wave attenuation is the presence of fluid in rocks. In this study, we estimated the attenuation structure in southwestern Japan and western Nankai trough by applying the attenuation tomography that takes account of apparent amplitude attenuation due to multiple forward scattering [Takahashi, 2012]. Because the estimated attenuation $1/Q$ in our tomographic study was much larger than $1/Q$ due to wide-angle scattering, our estimated $1/Q$ is composed mainly the intrinsic $1/Q$.

High $1/Q$ ($>1/500$ at 4-8 Hz) was imaged beneath the Quaternary volcanoes. The highest attenuation ($1/Q \sim 1/250$ at 4-8 Hz) distributes beneath the Beppu-Shimabara rift zone at 40-60km depth. Beneath this rift zone, $1/Q$ becomes larger as depth increases. Random inhomogeneities in this zone are relatively strong at 0-40 km depth; whereas at 40-60 km depth random inhomogeneities are almost comparable to those in non-volcanic area. Meanwhile, in northeastern Japan, uppermost mantle beneath the volcanoes shows strong inhomogeneities and high attenuation. Apparent attenuation at the uppermost mantle beneath the Quaternary volcanoes is high in both study areas, but relative contributions of scattering and intrinsic attenuation differ between northeastern Japan and the Beppu-Shimabara rift zone. If we consider random inhomogeneities and $1/Q$ in other areas, the weak random inhomogeneities and high $1/Q$ beneath this rift zone suggest that random inhomogeneities due to the presence of igneous rocks are not significant, and that any magma inclusions are too small to excite S-wave scattering at 4-32 Hz.

At off Shikoku region, moderate $1/Q$ ($1/800 \sim 1/1000$ at 4-8 Hz) is imaged at 0-20 km depth. This moderate $1/Q$ is estimated as $1/Q(f) \sim 10^{-2.5} f^{-0.5}$. Similar moderate attenuation can be found beneath the south of Shikoku at 20-40km, beneath the northern edge of Shikoku at 40-60km depth, and beneath Chugoku area at 40-60km depth. From geometry models of subducting Philippine Sea plate, most of the moderate $1/Q$ zone is located in and around the oceanic crust of subducting Philippine Sea plate except beneath Chugoku region. In this area, Shelly et al. [2006] pointed out fluid existence in the oceanic crust by estimating V_p/V_s structure. This correspondence implies this moderate $1/Q$ reflects fluid in the subducting slab. If we suppose that $1/Q$ of P- and S-wave have the same frequency dependences and that random inhomogeneities of P- and S-wave has the same scale dependences, we can show possible cases of fluid flow induced by the passage of low frequency seismic waves (<1 Hz) by applying a theoretical model of wave attenuation in saturated porous random media [Muller and Gurevich, 2005]. As a phenomenon suggesting such fluid flow by lower frequency seismic wave, triggering of non-volcanic tremors by surface waves passing has been observed [e.g., Miyazawa and Brodsky, 2008]. Even though we further need P-wave studies for detailed examination of this topic, it is likely that random inhomogeneity, intrinsic at 4-32 Hz and triggered tremors can be used to investigate medium properties and fluid dynamics.

秋田県森吉山周辺の地震活動：流体の移動との関連 Seismic activity near the Mori-yoshi-zan volcano in northeastern Japan: Implications for geofluid migration

小菅 正裕^{1*}
KOSUGA, Masahiro^{1*}

¹ 弘前大学理工学研究科
¹ Graduate School of Science and Technology

2011年東北地方太平洋沖地震によって、各地で誘発地震が発生した。その中で、秋田県森吉山周辺での地震活動は、地殻流体との関係において興味深いと考えて研究を行って来た。我々は、震源位置の精度を高めるために、2012年9月から臨時地震観測を行っている。観測点は、最も活発な地震クラスターの直上付近に1点、その7km程度北西の地点に9点から成るアレイ観測点を設置した。震源決定には、クラスター直上の1点と、アレイのうちの1点を用いた。これら臨時観測点のデータを加え、Double-difference法を用いて震源の再決定を行った。震源は顕著なマイグレーションを示し、そのパターンは複雑である。震源のマイグレーションを間隙流体圧の拡散によると解釈し、圧力源の位置と圧力増加が生じた時間、及び流体の拡散係数を、複数のマイグレーションに対して求めた。その結果、拡散係数として $0.01\sim 1.0\text{ m}^2/\text{s}$ の値が推定された。この値は、先行研究において水の圧入による誘発地震や自然地震から推定した値と調和的である。観測された地震波では、S波の後に顕著な後続波が見られる。これをS-S散乱波と仮定して、back-projection法で散乱源の位置を推定をした。その結果、散乱源は森吉山の北西約5km、深さ13km付近に存在することがわかった。この深さは、森吉山付近の深部低周波地震の震源深さの上限にほぼ対応する。森吉山周辺での地震活動は、東北地方太平洋沖地震から約2か月経過してから開始した。地震波の散乱源を流体の貯留する場所と考え、ここからの流体圧の拡散が東北地方太平洋沖地震直後に始まり、2か月経過して地震発生層の下限に達して地震活動を開始したと考え、拡散係数の値として $0.2\text{ m}^2/\text{s}$ 程度が推定される。これは上記の推定の範囲内に収まる。このことも、森吉山周辺での地震活動が地殻流体にトリガーされていることを示唆する。

キーワード: 東北地方太平洋沖地震, 誘発地震, 震源マイグレーション, 散乱, 地殻流体

Keywords: The 2011 Off the Pacific coast of Tohoku Earthquake, triggered seismicity, hypocenter migration, scattering, geofluid

地殻の電気伝導度は H_2O - NaCl 流体で説明できるか？ Is H_2O - NaCl fluid enough to explain high electrical conductivity in the earth's crust?

佐久間 博^{1*}; 市來 雅啓²
SAKUMA, Hiroshi^{1*}; ICHIKI, Masahiro²

¹ 物質・材料研究機構, ² 東北大学
¹National Institute for Materials Science, ²Tohoku University

古い大陸地殻では深さ 20 から 30 km に高電気伝導層が観測されている [1]。水流体 (aqueous fluid) の存在が、この高電気伝導層を説明するのではという仮説があり [2]、その仮説を検証するためには、高温高压条件における水流体の電気伝導度を知らなければいけない。地殻内の水流体は液体から超臨界状態に相当し、これらの状態での電気伝導度を知る必要がある。

実験的には電気伝導度の測定結果は、 NaCl 水溶液の場合、圧力 (P) < 400 MPa, 温度 (T) < 1073 K, 塩濃度 (c) < 0.6 wt% の低温低圧低塩濃度に限られている [3]。我々は古典分子動力学 (MD) 法を用いて、超臨界状態にある H_2O - NaCl 流体の電気伝導度を計算した。

超臨界状態の水を取り扱うため、我々が開発した H_2O 分子モデル (FIPC) [4] を使用した。計算の詳細は文献 [4] と同様である。本計算では塩濃度が 10 wt% 以下の H_2O - NaCl 流体について計算した。

電気伝導度の等温線を見ると、圧力の増加とともに電気伝導度も増加し、高压で飽和することが分かった。また温度の増加とともに電導度が減少することも分かった。これらの挙動は、温度圧力変化に伴う密度、イオンの動きやすさ、水の誘電率の変化で説明できる。

地殻のある圧力温度分布のモデルに沿って、電気伝導度の変化を計算すると、電磁気観測で見られる電気伝導度の変化のうち、 H_2O - NaCl 流体で電気伝導度の一桁の変化を説明できることがわかった。しかし観測で見られる 2 桁程度の電気伝導度の変化を説明するためには、流体の連結度や CO_2 の影響等を考量する必要があるようである。

References

- [1] T. J. Shankland and M. E. Ander (1983) *J. Geophys. Res.* **88** 9475-9484.
- [2] B. E. Nesbitt (1993) *J. Geophys. Res.* **98** 4301-4310.
- [3] A. S. Quist, and W. L. Marshall, (1968) *J. Phys. Chem.* **72** 684-703.
- [4] H. Sakuma, M. Ichiki, K. Kawamura and K. Fuji-ta (2013) *J. Chem. Phys.* **138** 134506.

キーワード: 塩水, 電気比抵抗, 超臨界流体, 分子動力学計算, 誘電率

Keywords: salt water, electrical resistivity, supercritical fluid, molecular dynamics, static dielectric constant

花崗岩中の空隙の連結度 Connectivity of cracks and pores in a granitic rock

渡辺 了^{1*}; 樋口 明良¹; 米田 明²

WATANABE, Tohru^{1*}; HIGUCHI, Akiyoshi¹; YONEDA, Akira²

¹ 富山大学大学院理工学研究部, ² 岡山大学地球物質科学研究センター

¹Graduate school of science and engineering, University of Toyama, ²Institute for Study of Earth's Interior, Okayama University

Seismic velocity and electrical conductivity are used to map the fluid distribution in the crust. Seismic velocity reflects the contiguity of solid phases, while electrical conductivity the connectivity of fluid phases. The combination of velocity and conductivity could provide us a strong constraint on the fluid distribution. However, mapping of the fluid distribution has not been successful. The connectivity of fluid phases in rocks is poorly understood. In order to understand the connectivity of fluid phases in rocks, we have made conductivity measurements on a fluid-bearing granitic rock under various confining pressures.

Fine grained (100-500 μ m) biotite granite (Aji, Kagawa pref., Japan) was used as a rock sample. The sample is composed of 52.8% plagioclase, 36.0% Quartz, 3.0% K-feldspar, 8.2% biotite. The density is 2.66(1) g/cm³, and the porosity 0.8(1) %. The porosity was estimated from the mass of the dry and wet samples. Cylindrical samples have dimensions of 25 mm in diameter and 30 mm in length, and saturated with 0.01 mol/l KCl aqueous solution. Simultaneous measurements of elastic wave velocity and electrical conductivity were made using a 200 MPa hydrostatic pressure vessel. The pore-fluid is electrically insulated from the metal work by using plastic devices (Watanabe and Higuchi, 2013). The confining pressure was progressively increased up to 125 MPa, while the pore-fluid pressure was kept at 0.1 MPa. It took five days or longer for the electrical conductivity to become stationary after increasing the confining pressure.

Elastic wave velocities and electrical conductivity showed reproducibly contrasting changes for a small increase in the confining pressure. Elastic wave velocities increased only by 5% as the confining pressure increased from 0.1 MPa to 25 MPa, while electrical conductivity decreased by an order of magnitude. The increase in velocities is caused by the closure of cracks. Most (~80%) of the decrease in electrical conductivity occurred below the confining pressure of 5 MPa. The decrease in electrical conductivity must also be caused by the closure of cracks. The decrease in porosity was only 0.07(1) %. Such a small change in porosity caused a large change in electrical conductivity. The connectivity of fluid was maintained at least up to the confining pressure of 125 MPa. A calculation with the effective medium theory (Kirkpatrick, 1973) suggests that the fluid forms a network with small coordination number (average coordination number=2.3), and that the connectivity at higher pressures is maintained by stiff pores. More cracks are open at lower pressures to link pores, drastically increasing electrical conductivity.

キーワード: 空隙, クラック, 連結度, 花崗岩, 電気伝導度

Keywords: pore, crack, connectivity, granitic rock, electrical conductivity

マントル捕獲岩中の粒間流体形状：岩石物性に対する効果 Geometry of intergranular fluids in the mantle xenoliths: Implications for the physical properties of upper mantle

中村 美千彦^{1*}; 奥村 聡¹; 吉田 武義¹; 佐々木 理²; 高橋 栄一³

NAKAMURA, Michihiko^{1*}; OKUMURA, Satoshi¹; YOSHIDA, Takeyoshi¹; SASAKI, Osamu²; TAKAHASHI, Eiichi³

¹ 東北大学大学院理学研究科, ² 東北大学総合学術博物館, ³ 東京工業大学大学院理工学研究科

¹Graduate School of Science, Tohoku University, ²Tohoku University Museum, ³Graduate School of Science and Engineering, Tokyo Institute of Technology

Recent magnetotelluric (MT) studies have revealed that crust and uppermost mantle are less resistive than dry rocks in various localities in the world. This suggests that interconnected fluid phases present more ubiquitously than previously realized. Intergranular fluids also decrease seismic wave velocities and changes Vp/Vs ratio, thus interpretation of the seismic tomographic images largely depends on the volume fraction and geometry of the fluid phase. The conventional view on grain-scale fluid distribution is based on dihedral angle between minerals and fluids in isotropic monomineralic rocks (i.e. ideal equilibrium geometry). Natural rocks are, however, composed of anisotropic multiple phases and undergo textural adjustment to minimize interfacial and strain energy such as grain growth and dynamic recrystallization, which results in microstructural complexity. In order to understand real fluid distribution in deep-seated rocks, we conducted an X-ray CT study of xenoliths from the uppermost mantle from various localities.

The mantle xenoliths samples investigated were from Ichinomegata (NE Japan), Eifel (W Germany), San Carlos (AZ, USA), Bullen Merri and Shadwell (Victoria, AU), Kilbourne Hole (New Mexico, USA), Longang-hu (NE China), Gi-rona (Spain), Lanzarote (Canary islands), and Moses Rocks (Utah, USA). The micro-focus X-ray CT imaging was performed using Comscantecno ScanXmate-D160TSS105 in Tohoku University Museum with a tube voltage of 100 – 130 kV and current of 90 – 120 mA. The voxel size was typically 43 – 73 μm^3 . The 3-D image analysis was carried out with a software package Slice[1].

All the observed spinel lherzolite and Harzburgite xenoliths contained up to a few vol% of intergranular pores, indicating that the rocks were saturated with a free-fluid phase. The imaged pore fluids are typically polyhedral and tens – hundreds of micrometers in scale; this suggests that they were formed via coalescence of smaller pore fluids. The fluids are localized in interphase boundaries (between different mineral phases), while most of the monomineralic triple junctions lack pore fluids. All these characteristics are consistent with the results of grain-growth experiments in a fluid-bearing biminerale system[2]; in other words, the role of interfacial energy anisotropy and grain growth are crucial in determining fluid distribution in nature. In the ellipsoid approximation, the 3-D shape of the intergranular fluids show deformed rugby-ball shape with aspect ratios larger than those of the equilibrium fluid geometry determined by the dihedral angle[3]. The geometry, distribution and thus connectivity of fluids cannot be assessed simply from dihedral angles.

The results of CT imaging suggest that no pervasive grain-scale fluid interconnection is established in the uppermost mantle. To explain the observed low electrical resistivity in the mantle which does not undergo partial melting, concentration (localization) and interconnection of CHO fluids in a larger spacing, such as in meter-scale shear zones should be necessary. Given the observed geometry of the inter-granular fluids, their effects on Vp/Vs ratio is limited.

References: [1] Nakano et al. <http://www-bl20.spring8.or.jp/slice/> (2006). [2] T. Ohuchi and M. Nakamura J. Geophys. Res. 111, B01201, doi: 10.1029/2004JB003340 (2005). [3] Y. Takei JGR 107 (B2) doi:10.1029/2001JB000522 (2002).

キーワード: マントル捕獲岩, 岩石微細構造, 弾性波速度, 電気比抵抗, 粒成長

Keywords: mantle xenoliths, rock microstructure, elastic wave velocity, electrical resistivity, grain growth

マントル起源かんらん岩捕獲岩中の鉍物境界に発達する微細組織観察 Ultra-fine textures along grain boundaries in nominally fresh mantle xenoliths

村田 雅美^{1*}; 植松 勝之²; 山本 貴史³; 谷 健一郎⁴; 宿野 浩司⁵; 水上 知行¹; 森下 知晃¹
MURATA, Masami^{1*}; UEMATSU, Katsuyuki²; YAMAMOTO, Takafumi³; TANI, Kenichiro⁴; SHUKUNO, Hiroshi⁵;
MIZUKAMI, Tomoyuki¹; MORISHITA, Tomoaki¹

¹ 金沢大学大学院, ² マリン・ワーク・ジャパン, ³ 広島大学大学院, ⁴ 海洋研究開発機構, ⁵ 無所属
¹ Kanazawa Univ., ² Marine Works Japan LTD., ³ Hiroshima Univ., ⁴ JAMSTEC, ⁵ non party

マントル物質中の結晶と結晶の境界(相境界)に、メルトや水に富む流体がどのように、どれだけ存在しているかは、メルトの発生や移動、マントルの物性・化学組成変動に直接的な影響を与えるため重要な情報である。実際に実験岩石学的、理論的アプローチは多い(例えば Drury, *geophysical research letters*, 1996, Hiraga et al., *nature article*, 2004)が、天然物質の観察例はほとんどない。

我々の研究グループでは、これまで知られていなかったマントル起源かんらん岩の結晶表面(相境界)のナノスケール微細組織に着目し、この組織が、固相-流体反応で相境界に形成された物質であると仮説をたて検証している。天然マントル物質を観察するためには、マントル起源の新鮮なかんらん岩と鉍物相境界を壊さないで観察する方法が必要である。かんらん岩捕獲岩は新鮮であるが、上昇時の体積増加のため鉍物相境界がはがれ、地表付近での低温低圧条件下で変質し、鉍物相境界の観察としては不十分である。そこで、新たな結晶表面観察・分析方法を確立し、天然かんらん岩試料に適用することが必要となっている。

本発表では、世界的に最も著名なかんらん岩捕獲岩の産地である米国アリゾナ州サンカルロスのかんらん岩捕獲岩での観察結果について予察的結果を報告する。先行研究では、このサンカルロスのかんらん岩捕獲岩結晶相境界にアモルファス相が報告されている(Wirth, *Contrib. Mineral. Petrol.*, 1996)。

鉍物境界を観察するには、一般的にTEMを用いた観察が主流であるが、できるだけ容易に多く観察したい。近年、電気を利用した鉍物分離装置(selFlag)が開発され、鉍物相境界を壊すことなく岩石を鉍物単位にばらばらにすることができるようになった。そこで、海洋開発研究機構のselFlagを用いて鉍物境界にそってばらばらにし、高空間分解能電子顕微鏡(FE-SEM)で観察した。

このかんらん岩捕獲岩の結晶表面の微細組織には多様性があり、以下のように分類した。(1) μm スケールで確認される組織(虫食い状組織や網目状の組織、自形のような物質、エッチピット)、(2) $<\mu\text{m}$ スケールの高空間分解能で観察される組織。(1)の μm スケールで確認される組織の上には、シート状の物質があり、その上に別の結晶が形成している場合もある。また、(1)の $>\mu\text{m}$ スケールで観察される組織であっても、(2)の $<\mu\text{m}$ スケール組織の集合体であるものも存在する。

現在、かんらん石結晶表面のEDS分析による化学組成の定性分析によって、表面を構成している物質の同定を行っている。かんらん石の(2) $<\mu\text{m}$ スケール組織は、 $<\mu\text{m}$ スケール組織が確認されない部分と比較するとMgよりもSiが多く、Alが含まれている。このことは、エッチピットの内部と外部でも同様で、内部と比較し外部はMgよりもSiが多く、Alが含まれている。また、シート状の物質や、自形のような形状の物質にはCaとSが含まれ、さらにNaとClからなる結晶もあった。また、今後透過型電子顕微鏡により結晶表面形態を観察する予定である。これらの結果から、相の同定や、形成条件、形成プロセスを報告する。

キーワード: かんらん岩捕獲岩, 微細組織, 透過型電子顕微鏡, 結晶相境界, 流体
Keywords: peridotite xenolith, Microstructures, TEM, grain boundary, fluids

下部一中部地殻条件下における元素輸送：三波川帯，塩基性片岩の吸水反応の例 Elemental transport under lower-middle crustal condition: example from hydration of basic schist, Sanbagawa belt, Japan

宇野 正起^{1*} ; 中村 仁美² ; 岩森 光³

UNO, Masaaki^{1*} ; NAKAMURA, Hitomi² ; IWAMORI, Hikaru³

¹ 東北大学大学院環境科学研究科, ² 東京工業大学大学院地球惑星科学専攻, ³ 海洋研究開発機構・地球内部物質循環研究分野

¹Graduate School of Environmental Studies, Tohoku University, ²Department of Earth and Planetary Sciences, Tokyo Institute of Technology, ³Geochemical Evolution Research Program, Japan Agency for Marine-Earth Science and Technology

To constrain the behavior of geofluids under the lower to middle crustal conditions, hydration reactions and trace element and Sr-Nd-Pb isotopic compositions of basic schists in the Cretaceous Sanbagawa metamorphic belt, a typical regional metamorphic belt in the circum-Pacific orogeny, have been investigated based on the observations of thin-sections and outcrops. The basic schists have undergone significant hydration from 0.8 GPa, 550 °C to 0.3 GPa, 400 °C during decompression towards the surface at the final stage of metamorphism. High-field-strength and rare-earth element compositions of the basic schists, as well as the Sr-Nd-Pb isotopic ratios, are different among three mineral zones with different peak P-T metamorphic conditions; the basic schists in the low-grade chlorite zone shows N-MORB-like compositions whereas those in the higher-grades, garnet and oligoclase-biotite zones, show more enriched compositions (E-MORB-like). On the other hand, there is a common feature to all the metamorphic zones; the enrichment degree of some group of elements (e.g., large-ion lithophile elements) relative to high-field-strength and heavy-rare-earth elements is proportional to loss on ignition that approximately measures the bulk rock H₂O content. This correlation suggests that Li, B, K, Cr, Ni, Rb, Sr, Cs and Ba have been added to the basic schists during hydration. The addition of these elements amounts to as much as 60-80% of the bulk abundance, indicating that significant amounts of elements were transported via pervasive fluid flow, which overprinted the variation in the bulk rock compositions of the protolith. The estimated compositions of hydration fluid show high concentrations in large-ion lithophile elements, lead and light-rare-earth elements (10-100 times denser than primitive mantle, Fig. 1) and are similar to those of the slab-derived fluids^[1] that induce arc volcanism. These elements (Cs, Rb, Ba, K, La, Ce and Pb) are thought to have been preferentially partitioned into the fluid when it was generated at depth. Such high concentrations indicate a high temperature origin of the hydration fluid, and are consistent with a model of hot slab subduction during exhumation of the Sanbagawa belt.

References:

[1] Nakamura, H., Iwamori, H., and Kimura, J.-I., 2008 *Nat. Geosci.*, **1**, 380-384

キーワード: 地殻流体, 変成作用, 微量元素, Sr-Nd-Pb 同位体, 吸水反応, 三波川変成帯

Keywords: geofluid, metamorphism, trace elements, Sr-Nd-Pb isotopes, hydration reaction, Sanbagawa metamorphic belt

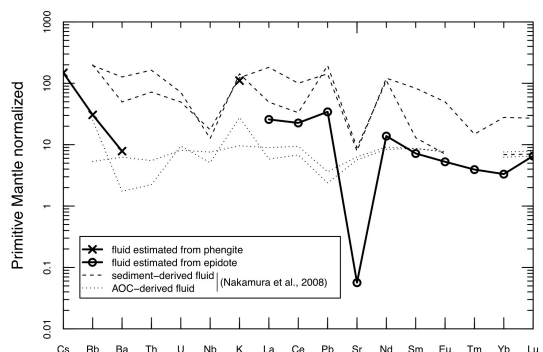


Fig. 1 Estimated compositions of the hydration fluid (solid lines). Compositions of slab-derived fluids estimated for arc volcanism (dotted lines; Nakamura *et al.*, 2008 *Nat. Geosci.*, **1**, 380-384) are shown for comparison. Note that the concentrations of LILE, Pb and LREE in the hydration fluid are in the range of slab-derived fluids.

マントルウェッジにおける蛇紋岩化作用の進行：酸化還元状態への影響 Progress of serpentinization in the mantle wedge and its effect on the redox state

小木曾 哲^{1*}; 三好 茜²

KOGISO, Tetsu^{1*}; MIYOSHI, Akane²

¹ 京都大学人間・環境学研究科, ²JX 日鉱日石エネルギー

¹Human Environ. Stds., Kyoto Univ., ²JX Nippon Oil & Energy Corporation

Serpentinization of peridotite in the mantle is a key process that significantly changes the physical properties of the mantle. Serpentinization also produces hydrogen, which is essential not only for the activity of microbial systems in hydrothermal fields on the seafloor, but also for controlling the oxidation state of the mantle in subduction zones. Hydrogen is generated along with the formation of magnetite during serpentinization. However, there still remains controversy about what factors promote the mineralogical reactions responsible for magnetite formation during serpentinization in natural ultramafic rocks. Recent petrologic studies have proposed that serpentinization reactions proceed via a two-stage process involving the early formation of serpentine and brucite and subsequent magnetite formation. Many studies proposed that magnetite forms by the break down of ferrous brucite promoted by the addition of aqueous silica, but others proposed that magnetite forms by the breakdown of ferrous serpentine which releases silica component. To solve this controversy, we examined a number of variably serpentinized harzburgite and dunite samples taken from the Iwanaidake ultramafic body in Kamuikotan belt, Japan (Miyoshi et al. 2014). Petrographic observations of these samples revealed that successive changes in textures, mineral chemistry, whole-rock H₂O contents, and magnetic susceptibility with the progress of serpentinization of harzburgite involved two stages: replacement of olivine by serpentine and brucite, and subsequent formation of magnetite along with more-magnesian serpentine and brucite. The later reactions occurred concurrently with serpentinization of orthopyroxene, which supplied the silica component. In serpentinized dunite, which doesn't contain orthopyroxene, serpentinization involved replacement of olivine by serpentine and brucite, and the fraction of magnetite did not increase with the progress of serpentinization. These observations, and the fact that the Iwanaidake ultramafic body originated from the forearc mantle of the Northeast Japan arc, suggest that the silica supply from serpentinization of orthopyroxene is an essential factor for the formation of magnetite during serpentinization in mantle wedge.

Our observations imply that serpentinization in the mantle wedge of subduction zone produces H₂ along with magnetite if sufficient amounts of silica component are supplied from subducting slab, which will probably occur because dehydration in subducted sediments can supply silica-rich fluids. Since H₂ is expected to exist as immiscible hydrogen-rich gas phases that coexist with H₂O fluids in normal subduction zone conditions, it will be rapidly migrate upwards owing to its very low density. Then the remaining serpentinites will become oxidized. Such oxidation associated with serpentinization would occur in the shallow part of the wedge corner where temperatures are lower than ~600 °C, but the oxidized (magnetite-bearing) serpentinite will be dragged downwards in the mantle wedge. Thus serpentinization reactions can be one of the main processes to increase the oxygen fugacity of the mantle wedge. On the other hand, the H₂ gas removed from the wedge corner will produce highly reduced fluid phases, which may result in reducing the shallowest part of the forearc mantle and the lower part of the forearc crust. This could be the cause of rare presence of metal phases in subarc peridotite.

Reference:

A. Miyoshi, T. Kogiso, N. Ishikawa, K. Mibe (2014) *American Mineralogist*, in press.

キーワード: 蛇紋岩化作用, 水素, 磁鉄鉱, 沈み込み帯, 酸化還元状態

Keywords: serpentinization, hydrogen, magnetite, subduction zone, redox state

石英脈形成に伴うき裂間隙構造の発達 Evolution of porosity structures in a fracture during quartz vein formation

山田 稜^{1*}; 岡本 敦¹; 最首 花恵¹; 中村 美千彦²; 奥村 聡²; 佐々木 理³; 土屋 範芳¹
YAMADA, Ryo^{1*}; OKAMOTO, Atsushi¹; SAISHU, Hanae¹; NAKAMURA, Michihiko²; OKUMURA, Satoshi²; SASAKI,
Osamu³; TSUCHIYA, Noriyoshi¹

¹ 東北大学大学院 環境科学研究科, ² 東北大学大学院 理学研究科, ³ 東北大学博物館

¹Tohoku university, ²Tohoku university, ³The Tohoku university museum

Ubiquitous occurrences of quartz veins suggest that dissolution/precipitation of silica provides significant effects on the hydrological and mechanical properties within the crust. For example, a model has been proposed that fracture sealing processes control the change of pore fluid pressure and thus earthquake cycle. Previous studies on natural quartz veins have focused on estimates of P-T conditions, stress and strain fields and fluid compositions; however, details of dynamics of fluid flow and how fractures are sealed during vein formation are still unclear. In this study, we synthesized quartz veins by the hydrothermal experiments, and observed the aperture structures by using X-ray CT to clarify how aperture structures evolve during vein formation.

We conducted the hydrothermal flow-through experiments for quartz precipitation from Si-supersaturated solutions under controlled high temperature and high pressure condition. The experimental apparatus consists of two vessels for preparation of the Si-supersaturated solution and for precipitation, respectively. The precipitation vessel has double-structure: the main flow path was the inner alumina tube (diameter=4mm), and the outer SUS tube was filled with static solutions. The advantage of this system is that we can take out the non-destructive sample for the X-ray CT analyses. We conducted two types experiments: first one is precipitation in porous media with alumina balls, the second one is rock slice as analog of a fracture.

In the alumina-ball experiments, we carried out the precipitation experiment at supercritical (430C, 30MPa) and vapor condition (370C, 20MPa). In both experiments, the significant silica precipitation within few days, but showed contrasting porosity structures. Under supercritical condition, amorphous silica was predominantly formed with covering the surfaces of the alumina balls and alumina tube, and discrete quartz crystal (50 μm) within the amorphous silica layers. The porosity (ϕ) gradually decreases with minimal porosity ($\phi = 0.4$) at $\sim 38\text{mm}$ from the inlet. In contrast, under vapor condition, fine-grained quartz grains (0.1-1 μm) were directly nucleated in solutions using surface of vapor, and immediately settled on the bottom. The porosity rapidly decreases from 18 mm ($\phi = 0.8$) to 25 mm ($\phi < 0.1$) from the inlet. These results suggest that a depressurization of crustal fluids related to fault dilation by earthquakes would cause a formation of fine-grained silica particles, and their mineralogy and transport/deposition properties strongly depend on properties water.

In the experiment with rock slits, we evaluated the effect of rock substrate (amount and distribution quartz in the fracture wall). The P-T conditions and solution chemistry are similar to the previous experiments, but we used granite core with a slit ($\sim 300 \mu\text{m}$). The mineralogy and aperture structures changes systematically along the fluid flow path. From the inlet to 35 mm of fracture, nucleation of quartz and other silica polymorphs predominantly occurred, regardless of vein wall minerals. From $>35\text{mm}$ low Si concentration, silica precipitates occurred as epitaxial overgrowth from quartz crystal. The wavelength of aperture structures is controlled by distribution and grain size of quartz of the host granite. Accordingly, fractures are not sealed homogeneously, but complex flow pathways are evolved during vein formation. Such a variation in the precipitation mechanism and porosity structures during quartz vein formation may affect the evolutions of permeability and strength of rock fractures in the Earth's crust.

Keywords: Hydrothermal experiments, Quartz, Vein, Fracture, Porosity

LAL-ICPMS法を用いた局所高精度Pb同位体分析による熱水性方鉛鉱の起源推定 High precision in situ Pb isotope analysis of galena by LAL-ICPMS technique

若木 重行^{1*}; 谷水 雅治¹
WAKAKI, Shigeyuki^{1*}; TANIMIZU, Masaharu¹

¹ 海洋研究開発機構 高知コア研究所

¹ Kochi Institute for Core Sample Research, JAMSTEC

Radiogenic Nd and Pb isotopic compositions of the fluids originated from subducting Pacific and Philippine Sea plates have been characterized from isotopic trends observed among arctic volcanic rocks (Nakamura et al., 2008). Origin and evolution of the fluids that produced hydrothermal ore deposits may now be investigated by radiogenic isotopic compositions of ore deposits. In this study, we analyzed the micro scale isotopic variation of Pb in a hydrothermal galena to shed light on the macro scale dynamics of the fluids. To investigate the possibly small degree of isotopic changes within a galena sample, both high spatial resolution and high precision are required for the isotopic analysis. We employed the combination of laser ablation in liquid (LAL) micro sampling technique (Okabayashi and Hirata, 2011) and solution-based Pb isotopic analysis by MC-ICPMS technique to meet the analytical requirements. In the LAL micro sampling, laser-ablated sample particles are trapped in the liquid that placed above the sampling area. The trapped samples are then dissolved and introduced to the ICPMS as a solution. The advantage of the combined LAL-ICPMS technique over laser ablation (LA) ICPMS technique is the stable ion signals due to solution form, which allows high-precision isotope ratio measurement.

Sample analyzed in this study was a hydrothermal galena from Hosokura mine (Miyagi, Japan). A microscopic texture of the sample was observed in detail with FE-SEM-EDS system (JEOL JSM-6500F) prior to the isotopic analysis. A fs laser (IFRIT, Cyber Laser, Japan) with a wavelength of 780 nm (~200 fs pulse width) was used for the LAL micro sampling. Care was taken to avoid sampling of grain boundaries and inclusions. Typical spatial resolution was 150 micron in diameter and 30 micron in depth. The laser-sampled PbS (300-400ng Pb) trapped in Milli-Q water was dissolved in conc. HNO₃, and adjusted to 200 ng/mL Pb solution in 0.15 M HNO₃ for Pb isotopic analysis. Pb isotope ratios were determined with a MC-ICPMS, Neptune (Thermo Instruments, Bremen, Germany). An isotopic reference material of Tl (NIST-SRM 997) was added to the final sample solutions for the correction of mass discrimination of Pb in the instrument to have a concentration of 20 ppb Tl.

Galena occurs as discrete layers of ca. 1cm width in between layered CaF₂ as well as sub mm-sized inclusion within thick CaF₂ layer. Galena inclusion and layers were numbered from 1 to 3 according to its precipitation order. Grain size of the galena in each of the layer is several hundred microns to several millimeters. Euhedral quartz with a size of 10-100 micron occurs along the grain boundary of galena and as an inclusion within galena grains.

Small but significant Pb isotopic variation of sub-permil order was observed among and within the 3 galena layers. The analyzed samples clearly form a linear trend in the ²⁰⁸Pb/²⁰⁷Pb vs. ²⁰⁶Pb/²⁰⁷Pb diagram. The observed Pb isotopic trend indicates that the Pb isotopic composition of the fluid that produced the galena has slightly changed during galena precipitation. The Pb isotopic composition of the galena is consistent with mixing of a sediment component of the Pacific plate (Nakamura et al., 2008) with a deep fluid derived from Pacific Ocean plate (Nakamura et al., 2008) and/or the DMM. With the high-precision isotopic analysis as demonstrated in this study, LAL-ICPMS may have an important contribution to high-spatial-resolution geochemical studies in the future.

キーワード: 地殻流体, LAL法, Pb同位体比, 方鉛鉱, 局所同位体分析

Keywords: Geofluids, laser ablation in liquid, Pb isotope ratio, galena, in situ isotope analysis

中央構造線沿いに湧出する高塩分泉の起源 —プレート脱水流体起源の可能性についての水文化学的検討—
Origin of saline waters distributed along the Median Tectonic Line in southwest Japan

網田 和宏^{1*}; 大沢 信二²; 西村 光史³; 山田 誠⁴; 三島 壮智²; 風早 康平⁵; 森川 徳敏⁵; 平島 崇男⁶
AMITA, Kazuhiro^{1*}; OHSAWA, Shinji²; NISHIMURA, Koshi³; YAMADA, Makoto⁴; MISHIMA, Taketoshi²; KAZAHAYA, Kohei⁵; MORIKAWA, Noritoshi⁵; HIRAJIMA, Takao⁶

¹ 秋田大学大学院工学資源学研究科地球資源学専攻, ² 京都大学大学院理学研究科附属地球熱学研究施設 (別府), ³ 東洋大学 経済学部, ⁴ 総合地球環境学研究所, ⁵ 産業技術総合研究所地質情報研究部門, ⁶ 京都大学大学院理学研究科地球惑星科学専攻

¹Department of Earth Science & Technology Faculty of Engineering and Resource Science Akita University, ²Institute for Geothermal Sciences, Graduate School of Science, Kyoto University, ³Faculty of Economics, Toyo University, ⁴Research Institute for Humanity and Nature, ⁵Geological Survey of Japan, AIST, ⁶Department of Geology and Mineralogy, Graduate School of Science, Kyoto University

温泉起源流体としての変成流体を探索するために、西南日本の前弧域の中央構造線沿いに湧出する高塩分温泉において、温泉水や付随ガスを採取し化学・同位体分析を行った。その結果、和歌山と四国地域で採取した温泉水試料から、現海水や浅層地下水に比べて水素・酸素安定同位体組成の大きく異なる温泉を見出した。四国地域の温泉起源流体は、Li-B-Cl 相対組成や He 同位体システムティクスから、続成流体の一つであることが確認された。一方、和歌山地域の温泉起源流体は、続成脱水流体とは異なる Li-B-Cl 相対組成を示し、また高い ³He/⁴He 比を有していることから、大分平野で得られたものと同様、その起源が変成脱水流体にあると判断された。和歌山、大分の温泉起源流体と四国、宮崎のそれでは、付随ガスの化学組成において前者が CO₂ に富むのに対して後者は CH₄ に富むという明瞭な違いが認められ、また、和歌山と大分の付随ガスに含まれる CO₂ の大半が、沈み込み帯の火山ガスと同様に、海成炭酸塩に由来するものであることが示された。さらにこれら起源流体の Li-B-Cl 相対組成は、続成脱水流体と火山性熱水流体のその中間的な値を示した。これらの結果は全て、和歌山と大分の温泉起源流体が、沈み込むフィリピン海プレートより脱水してきた変成脱水流体であることを示唆しているものと考えられた。

キーワード: 温泉水, プレート脱水流体, 中央構造線

Keywords: hot spring water, dehydrated fluid from subducting plate, Median Tectonic Line

東北日本のヘリウム同位体比分布；地質構造との比較 Distribution of the helium isotope ratios in northeast Japan in terms of geological setting

堀口 桂香^{1*}；風早 康平¹；塚本 齊¹；森川 徳敏¹；佐藤 努¹；大和田 道子¹；仲間 純子¹
HORIGUCHI, Keika^{1*}；KAZAHAYA, Kohei¹；TSUKAMOTO, Hitoshi¹；MORIKAWA, Noritoshi¹；SATO, Tsutomu¹；
OHWADA, Michiko¹；NAKAMA, Atsuko¹

¹ 産業技術総合研究所 地質情報研究部門

¹ Geological Survey of Japan, AIST

The distribution of slab fluid defined by high Li/Cl ratios conforms the area of "hot fingers" (Tamura et al., 2002) in Northeast Japan (Kazahaya et al., submitted). Conversely, the high $^3\text{He}/^4\text{He}$ ratios distribute wider and do not match with slab-derived fluids indicating that some of the mantle-derived helium would not be transported with magmas or slab fluids but directly upwells as mantle-derived fluid. The $^3\text{He}/^4\text{He}$ ratios vary along the volcanic front showing an areal contrast; such as a low-ratio-area close to volcanoes are observed in the central part of Tohoku. We propose here an extended helium upwell model which can explain the spatial variation of $^3\text{He}/^4\text{He}$ ratios with the following concept; 1) The most important constraint for mantle helium upwelling is the crustal structure divided by tectonic lines; Hatagawa Tectonic Line (HTL) divides the Kitakami and Abukuma belts. Ryoke belt and north part of Abukuma belt is torn apart by number of faulting events. The rest of parts, Abukuma granitic province and Kitakami province form very large stable blocks which might prohibit helium to upwell from mantle. 2) A view from U-Th content in the crust is important to understand the flat distribution of mantle helium in back-arc region; Low U-Th crust in the back-arc with less crustal ^4He production is favorable to explain the flat and high $^3\text{He}/^4\text{He}$ signature, such as oceanic crust might have. Tanakura Tectonic Line (TTL) divides the thick crust of continental margin (sedimentary prism and granite) with Ryoke belt.

キーワード: ヘリウム同位体比, 東北日本, 空間分布, 地質構造

Keywords: helium isotope ratio, northeast Japan, areal distribution, geological structure

地下水中に含まれるスラブ流体の新指標：塩水のLi-Cl-Br関係 The Li-Cl-Br systematics of saline groundwater: A new indicator for slab fluid

風早 康平^{1*}; 高橋 正明¹; 岩森 光²
KAZAHAYA, Kohei^{1*}; TAKAHASHI, Masaaki¹; IWAMORI, Hikaru²

¹ 産業技術総合研究所地質情報研究部門, ² 海洋研究開発機構・地球内部物質循環研究分野

¹Geological Survey of Japan, AIST, ²Geochemical Evolution Research Program, Japan Agency for Marine-Earth Science and Technology

In this study, we propose Br/Cl ratio as a new indicator for slab-derived fluids, which is useful to distinguish their sources between pore water and hydrous minerals in subducting slab. The areal distribution of slab-derived fluids and their sources using Li/Cl and Br/Cl as geochemical evidences will provide a view for water circulation in subduction zones.

Subducting slab contains waters (originally seawater) as pore water and many kinds of hydrous minerals. Hydrous minerals such as opal, clay or mica will decompose to release water during subsiding, and pore water will be released by compaction. Even though such complex process occurs, behavior of halogen ions in the subducting slab may be simple because they are always enriched in aqueous phase (pore water) and the rest are in minerals as a replacement of OH. Some metamorphic fluids in wedge mantle peridotite with Br-enriched signature have been observed and were indicated to be from pore water in the slab. The mineral dehydration process is supposed to be responsible for Br-depletion in slab-derived aqueous fluid. Therefore, halogens are potentially good indicators concerning with the water behavior in subduction processes.

The higher Br/Cl ratios (>0.0035 in wt.) have been observed in fossil seawater and oil field brines due to the addition of Br from organic matters. The very low Br/Cl waters (<0.0025 in wt.) have feature of ¹⁸O-shift to the slab (magmatic) fluid end member, which is quite lower than that in seawater (Br/Cl = 0.0034 in wt.), indicating that these waters originate from dehydration of the slab.

キーワード: Li-Cl-Br, スラブ起源流体, 地下水, 沈み込み帯

Keywords: Li-Cl-Br, slab-derived fluid, groundwater, subduction process

沈み込み帯の火山岩における U-Th 放射非平衡の起源 Origin of U-Th disequilibrium in subduction zone volcanic rocks

横山 哲也^{1*}; 池本 昭彦¹; 岩森 光²; 上木 賢太¹
YOKOYAMA, Tetsuya^{1*}; IKEMOTO, Akihiko¹; IWAMORI, Hikaru²; UEKI, Kenta¹

¹ 東京工業大学地球惑星科学専攻, ² 海洋研究開発機構

¹Department of Earth and Planetary Sciences, Tokyo Institute of Technology, ²JAMSTEC

Subduction zone magmatism is induced by the addition of slab derived fluids to the mantle wedge [1]. Chemical compositions of subduction zone volcanic rocks are largely controlled by the chemical and physical properties of the slab fluid. The nature of slab fluids have been extensively studied by geochemical approach utilizing trace element abundances and isotope compositions in arc basalts [2]. U-series disequilibrium in arc volcanic rocks is a useful tracer to understand the origin of arc magmas as well as the timescales of fluid/melt migration in subduction zones. However, detail of the process that producing ^{238}U - ^{230}Th disequilibrium in primary melts in the mantle wedge is still poorly constrained.

In this study, we determined ^{238}U - ^{230}Th disequilibrium in volcanic rocks from the Northeast Japan Arc (Iwate, Akitakoma, Yakeyama, Hachimantai, and Kampu). In addition, we performed a numerical simulation that reproduced ($^{238}\text{U}/^{232}\text{Th}$) and ($^{230}\text{Th}/^{232}\text{Th}$) ratios in primary melts in a subduction zone, by simultaneously calculating mantle dynamics, hydro phase reactions and trace elements transport. To discuss the origin of U-Th disequilibrium in arc volcanic rocks, the new data and previously published U-Th data around Japan were evaluated based on the result of the numerical simulation. The numerical simulation performed in this study

Most of arc volcanic rocks possess ^{238}U - ^{230}Th disequilibrium with 238U excesses, suggesting the addition to the mantle wedge of slab fluid enriched in U relative to Th. The feature of ^{238}U enrichment is well reproduced by the numerical simulation. Interestingly, the simulation produced two positive trends in the U-Th diagram; the shallow trend matches data from the Izu-Mariana arc, while the steep slope is consistent with data from the Kamchatka arc. This strongly suggests that the positive trend in the U-Th diagram for a single arc samples simply reflects the variation of ($^{238}\text{U}/^{232}\text{Th}$) and ($^{230}\text{Th}/^{232}\text{Th}$) ratios in primary melts produced in the mantle wedge, and the slope does not have any age significance. Thus, as discussed in [3], the decoupling of U-Th and Th-Ra ages for arc samples would be explained by assuming that the slab derived fluid have ($^{230}\text{Th}/^{232}\text{Th}$) ratios higher than the mantle wedge composition.

Although the NEJ frontal-arc lavas (Iwate) possess ^{238}U - ^{230}Th disequilibrium with ^{238}U excesses, the extent of 238U enrichment is moderate (<10%) compared to the other frontal-arc samples. In addition, Iwate lavas have relatively low ($^{230}\text{Th}/^{232}\text{Th}$) ratios that cannot be explained by the numerical simulation. This implies that the ($^{230}\text{Th}/^{232}\text{Th}$) in mantle wedge beneath Iwate volcano is lower than that in the depleted MORB mantle (DMM), due presumably to ancient mantle metasomatism by Th-enriched fluids derived from sediments.

In contrast to the frontal arc samples, the extent of ^{238}U enrichment in the NEJ samples decreases as the slab depth increases, and the rear-arc lavas (Kampu) show 230Th enrichments relative to ^{238}U (<10%). This generally reflects gradual decrease of the amount of slab derived fluid mixed into the wedge mantle. The ^{230}Th excesses in rear-arc lavas would be produced by the melting of garnet-bearing upwelling mantle, as reproduced by the simulation. However, our data for Kampu show 230Th excesses with an extremely low ($^{230}\text{Th}/^{232}\text{Th}$) ratio (~0.8) that plots outside the simulation data. This is explained by assuming the existence of metasomatized mantle beneath the NE Japan as discussed above, although the possibility of direct addition of Th-enriched fluid to the DMM-like mantle cannot be ruled out for the generation of rear-arc magmas.

References: [1] Iwamori (1998) *EPSL* 160, 65. [2] Nakamura et al. (2008) *Nature Geosci.* 1 380. [3] Yokoyama et al. (2003) *JGR* doi: 10.1029/2002JB002103.

キーワード: U-Th 放射非平衡, 沈み込み帯, 火山岩, スラブ由来流体

Keywords: U-Th disequilibrium, Subduction zone, volcanic rocks, slab derived fluid

沈み込み帯深部の水循環とマントル対流との相互作用 Water transport coupled dynamically with a plate-mantle convection system involving a shallow to deep subduction zone

中久喜 伴益^{1*}; 金子 岳郎¹; 中尾 篤史²; 岩森 光³
NAKAKUKI, Tomoeki^{1*}; KANEKO, Takeo¹; NAKAO, Atsushi²; IWAMORI, Hikaru³

¹ 広島大学大学院理学研究科地球惑星システム学専攻, ² 東京工業大学大学院理工学研究科地球惑星科学専攻, ³ 海洋研究開発機構・地球内部物質循環研究分野

¹Dept. Earth and Planetary Systems Science, Hiroshima Univ., ²Dept. Earth and Planetary Sciences, Tokyo Inst. Technology, ³Geochemical Evolution Research Program, JAMSTEC

水がマントル岩石の融点を下げ、部分融解を作り出すことは、島弧の火成活動に不可欠であると考えられている。島弧下のマントルの流動と水輸送を結合した数値モデリングにより、スラブが脱水してから部分融解の生成に至るまでの過程を詳しく理解できるようになった (Iwamori, 1998; 2007)。一方、背弧や大陸プレート内部においても、火山活動が見られることや、リソスフェアが大きく変形し、表層に厚い地震波高速度域が見られないことから、沈み込んだスラブからの水が影響を与えている可能性があると考えられる。それでは、沈み込み帯深部に沈み込んだスラブから水がどのように発生し、また、水は沈み込み帯のダイナミクスにどのような影響を与えるのであろうか。これらの動力学的過程を理解するため、沈み込み帯深部までの水輸送とプレートの沈み込みを動的結合したマントル対流の数値モデルを構築し、シミュレーションを行った。

基礎となるモデルとして、これまで著者らが開発してきた自発的沈み込みのモデル (Tagawa et al. 2007; Nakakuki, et al. 2010) を使用した。このモデルに、含水鉱物の相図 (Iwamori, 1998; 2007) と水輸送を組み込む。岩石の最大含水量は相図から決まる水和鉱物・結晶内の水だけでなく、結晶粒界の水も考慮した。水がマントル対流に与える影響として、含水によって岩石の密度や粘性が低下する効果 (Karato and Jung 2003) を考える。最大含水率を超えると岩石は脱水し、その水は浸透流により上方に運ばれると考えられる。その速度は、マントル対流よりも大幅に高速であると考えられるので、脱水した水は瞬間的に上方へ動くことと仮定して、その移動をモデルに取り入れた。水の拡散はマントル対流の時空間スケールよりも無視できるほど小さいので、水の輸送は拡散項のない移流方程式で表されることになる。拡散のない式をEuler的な方法で解くのは難しいため、マントル対流に伴って移動する水の移流方程式の解法に Marker-And-Cell (MAC) 法を適用した。脱水を計算する際、メッシュと粒子の間で水含有率を交換する必要がある。このとき、脱水した水をメッシュ内の粒子に分配する扱いを工夫し、水が玄武岩と橄欖岩との間で拡散するのを極力抑えた。

岩森らの研究や地震学的な研究 (Kawakatsu and Watada, 2007) によると、海洋地殻から脱水した水は、スラブ上面の橄欖岩に取り込まれ serpentine あるいは chlorite として、150km 程度の深さまで輸送される。我々のモデルでは、この含水層が安定に形成されるためには、沈み込む海洋地殻の含水量は 2% 程度以上でなければならなかった。また、強度については、プレート境界の逆断層と同程度かそれよりも小さくしなければならなかった。これらは Horiuchi (2013) の結果と調和的である。この相が choke point で分解した後、水は高温のマントルへ脱水し、高温の nominally anhydrous minerals (NAMs) により深部へ輸送される。このとき、NAMs が持つことの出来る水は最大で 0.2 wt. % 程度と推定される。これより大きい場合 (0.4 wt. %) には、深部へ輸送される水が多くなりすぎて島弧下のマントルを水で満たすことは出来なくなってしまう。岩石の相図から予想されるように、NAMs は脱水することなく、マントル遷移層に沈み込む。Richards and Iwamori (2010) は水平なスタグナントスラブが形成された際、含水層がレイリー・テイラー不安定を起こし、プルームとして上昇する可能性を示した。これに対し本研究では、そのような不安定の発生は見られなかった。一方、下部マントルに沈み込むスラブは、下部マントルの含水量に依存して脱水する。下部マントルの含水量が 410km 以浅の NAMs マントルより小さい場合には脱水を起こす。この場合、スラブ上面の含水層は 660km 相境界面を境に大きく水平方向へ広がることが分かった。これは、上方への脱水とマントル対流に伴う斜め下降を繰り返すためである。脱水した水によって、水に飽和した薄い層が 660km 相境界直上に形成された。この層は軽いので、不安定となり、含水プルームとして上昇し始める。410km の相境界より上部では、含水量が遷移層よりも小さい。このため、含水プルームは 410km 境界に達すると水を放出する。放出された水は、島弧下の水輸送と同様、浸透流として上昇する。その浸透流は、含水プルームの大きさによっては上盤プレートにまで達することも見られた。このような機構により、背弧側リソスフェア下のウェッジマントルには大量の水が運ばれ、島弧から 500 から 1000km 程度の範囲が 1 億年程度の時間で水に満たされた。含水プルームと背弧側プレートの相互作用は、リソスフェア下部を浸食するため、時間が経過しても背弧リソスフェアを薄いまま保つことが出来る。この作用により、含水プルームは背弧に部分融解を引き起こすだけでなく、島弧下のアセノスフェアを高温に保つ機構としても働くことが分かった。

SIT40-17

会場:416

時間:5月1日 15:45-16:00

キーワード: 沈み込み帯, 水輸送, 遷移層, スラブ, 含水プルーム, マントル対流

Keywords: subduction zone, water transport, transition zone, slab, hydrous plume, mantle convection

浅部ゆっくり地震活動と地殻流体に基づく地殻変動とプレート間固着の特徴とまとめ

An overview of seismic coupling and crustal deformation on the basis of geofluid and shallow slow earthquakes

有吉 慶介^{1*}; 松澤 暢²; 日野 亮太³; 長谷川 昭²; 堀 高峰¹; 中田 令子¹; 金田 義行¹
ARIYOSHI, Keisuke^{1*}; MATSUZAWA, Toru²; HINO, Ryota³; HASEGAWA, Akira²; HORI, Takane¹; NAKATA, Ryoko¹; KANEDA, Yoshiyuki¹

¹ 海洋研究開発機構 地震津波・防災研究プロジェクト, ² 東北大学大学院理学研究科附属地震・噴火予知研究観測センター, ³ 東北大学災害科学国際研究所

¹ Japan Agency for Marine-Earth Science and Technology (JAMSTEC), ² Research Center for Prediction of Earthquakes and Volcanic Eruptions, Tohoku University, ³ International Research Institute of Disaster Science, Tohoku University

本発表では、地殻流体の役割として、高間隙圧による浅部ゆっくり地震への寄与に関する研究のまとめを行う。

浅部超低周波地震は、これまで西南日本や十勝沖でしか捉えられてこなかったが、東北地方太平洋沖地震後の詳細な解析により、東北沖でも発生していることが確かめられた。そこで本研究では、数値シミュレーションに基づいて、浅部超低周波地震の活動とプレート間固着との関係を調べ、その結果を東北地方太平洋沖地震へ適用することを試みた。

南海トラフ沿いで発生する”ゆっくり地震”の一種である超低周波地震は、30kmの等深線上にほぼ分布しているだけでなく、海溝付近でも発生していることが、最近の海底観測から明らかとなった。

そこで本発表では、海溝まで地震性すべりが突き抜けるほど強く固着する場合と地震性すべりが海溝まで突き抜けにくい弱い固着の場合について、大規模な数値シミュレーションの計算結果を比較し、浅部超低周波地震の活動変化の特徴およびそれに伴う地殻変動についての抽出を試みると共に、地殻流体の役割について西南日本と東北沖とで比較しながら議論する予定である。

キーワード: 海溝型巨大地震, 沈み込み帯, 地震の静穏化, 高間隙圧, 海底観測, 速度状態依存摩擦構成則

Keywords: megathrust earthquake, subduction zone, seismic quiescence, high pore pressure, seafloor observation, rate- and state-dependent friction law

九州地方の三次元 P 波減衰構造 Three-dimensional seismic attenuation structure beneath Kyusyu

才田 悠人^{1*}; 中島 淳一¹
SAITA, Hiroto^{1*}; NAKAJIMA, Junichi¹

¹ 東北大学
¹Tohoku University

1. はじめに

九州地方では、フィリピン海プレートの沈み込みによる活発な島弧火山活動がみられる。さらに、阿蘇と霧島との間におよそ 110 km の火山空白域があるなど火山分布に興味深い特徴もある。島弧マグマの生成・上昇過程に関しては、多くの沈み込み帯において、地震波速度構造などに基づいたモデルが提唱されている（たとえば、Hasegawa and Nakajima, 2004）。一方、地震波減衰は、温度異常や流体分布に対して、地震波速度とは異なる影響をうけることが知られている。そのため、地震波減衰構造を詳細に推定することは、プレート沈み込みに起因するマントルウェッジの物理プロセスを理解するうえで重要である。本研究は、九州地方の詳細な 3 次元減衰構造を推定し、九州地方のマグマ生成・上昇のメカニズムの理解を深めることを目的とする。

2. データ・解析手法

本研究では、Nakajima et al. (2013) の手法を、2003 年 4 月から 2013 年 12 月までに九州地方とその周辺で発生した 5195 個の地震の速度変位スペクトルに適用した。まず、S コーダ波のスペクトル比法によって震源パラメータを求め、その震源パラメータを用いて観測された P 波速度振幅スペクトルを補正した。次いで、補正したスペクトルをデータとして、観測点毎に観測方程式を立て、インバージョンにより波線に沿った減衰 (t^*)、サイト増幅特性とスペクトルレベルとを同時に推定した。結果として 75207 本の t^* が得られた。最後に、得られた t^* をインバージョンすることで 3 次元 P 波減衰構造を推定した。

3. 結果と議論

得られた結果の特徴を以下に示す。

- 1) 深さ 10km では活火山直下が高減衰異常を示す。
- 2) 下部地殻では九州全域が比較的高減衰を示す。この結果は、火山直下のみで高減衰を示す東北地方の結果とはやや異なっている。
- 3) 沈み込むフィリピン海プレートは非常に減衰が小さい。
- 4) 背弧側のマントル上昇流に対応すると考えられる領域が高減衰を示す。しかし、阿蘇、霧島の間が存在する火山空白域にはマントル上昇流に対応する高減衰域は見られな。

今後は、解の分解能の評価を行うとともに、得られた 3 次元減衰構造と速度構造など他の結果と比較し、九州地方のマグマ上昇モデルを提案する予定である。

キーワード: 地震波減衰構造, フィリピン海プレート, 九州
Keywords: seismic attenuation structure, Philippine Sea Plate, Kyusyu

磁場変換関数データによる九州地方の3次元比抵抗構造 3D Electrical Resistivity Imaging beneath Kyushu by Geomagnetic transfer function data

畑 真紀^{1*}; 上嶋 誠¹; 半田 駿²; 下泉 政志³; 田中 良和⁴; 橋本 武志⁵; 鍵山 恒臣⁴; 歌田 久司¹; 宗包 浩志⁶; 市來 雅啓⁷; 藤田 清士⁸

HATA, Maki^{1*}; UYESHIMA, Makoto¹; HANDA, Shun²; SHIMOIZUMI, Masashi³; TANAKA, Yoshikazu⁴; HASHIMOTO, Takeshi⁵; KAGIYAMA, Tsuneomi⁴; UTADA, Hisashi¹; MUNEKANE, Hiroshi⁶; ICHIKI, Masahiro⁷; FUJI-TA, Kiyoshi⁸

¹ 東京大学地震研究所, ² 佐賀大学農学部, ³ 九州職業能力開発大学校, ⁴ 京都大学理学研究科, ⁵ 北海道大学大学院理学研究院附属地震火山研究観測センター, ⁶ 国土地理院, ⁷ 東北大学大学院理学研究科, ⁸ 大阪大学院工学研究科

¹Earthquake Research Institute, the University of Tokyo, ²Faculty of Agricultural Science, Saga University, ³Kyushu Polytechnic College, ⁴Graduate School of Science, Kyoto University, ⁵Institute of Seismology and Volcanology, Graduate School of Science, Hokkaido University, ⁶Geographical Survey Institute, ⁷Graduate School of Science, Tohoku University, ⁸GSE, Osaka University

The Kyushu island in the Southwest Japan Arc has many Quaternary active volcanoes in relation to the subduction of the Philippine Sea Plate (PSP). The volcanoes exist along the volcanic front of N30°E-S30°W, whereas the volcanoes are densely located in the northern and southern regions of the island. The Kyushu island has a non-volcanic region in the central region of the island between the two volcanic regions. We performed three-dimensional (3D) inversion analyses to obtain a lithospheric-scale electrical resistivity model beneath the entire Kyushu island using the Network-Magnetotelluric (MT) data. The electrical resistivity model, however, has a limited resolution in a horizontal direction because of the sparse Network-MT data in several areas of Kyushu. Thus data of geomagnetic variations are used anew to improve the uncertainty of the electrical resistivity structure in a horizontal direction. Data of geomagnetic variations were obtained at the entire Kyushu island and several islands off the western coast of Kyushu from 1980's to 1990's [e.g., Handa et al., 1992; Shimoizumi et al., 1997; Munekane et al., 1997]. In this study, accessible data of geomagnetic variations around Kyushu are compiled. Geomagnetic transfer functions for the data of geomagnetic variations in the northern Kyushu are re-estimated using the BIRRP code [Chave and Thomson, 2004] in order to enhance the quality of the transfer functions and their error estimation. The transfer functions at about 150 sites, which are 12 periods between 20 and 960 s, are obtained with improving quality at the entire Kyushu island. The induction vector representation [Parkinson, 1962] is generally used to delineate the lateral variation of electrical resistivity structure because the vectors point to current concentration in conductive anomalies. Induction vectors determined using the improved transfer functions have the following specific features. First, the vectors on the northern and central Kyushu do not point to the Pacific ocean off the eastern coast of Kyushu but point to the East China Sea of the shallow sea off the western coast of Kyushu. Second, the induction vectors on the southern Kyushu point to the Pacific ocean in the eastern part and point to the East China Sea in the western part at short period, whereas the vectors are arranged along a direction parallel to a direction of the coast line at longer period (>300 s). These results are consistent with the previous work [Handa et al., 1992; Shimoizumi et al., 1997; Munekane, 2000]. It is considered that the complex behavior of the induction vectors are influenced by conditions of the Earth's mantle relating to the igneous activities. Then we applied three-dimensional (3D) inversion analyses for geomagnetic transfer functions using the WSINV3DMT inversion code [Siripunvaraporn and Egbert, 2009]. The electrical resistivity of a starting model is based on values of the 3D electrical resistivity model estimated by using the Network-MT data. In this presentation, we will mainly describe features of the 3D electrical resistivity structure using the geomagnetic transfer functions and them of the 3D electrical resistivity structure using only the Network-MT data [Hata et al., 2013].

含水岩石の弾性波速度・電気伝導度に対する封圧・間隙流体圧の影響 Influence of confining and pore-fluid pressures on velocity and conductivity of a fluid-saturated rock

瀬間 文絵^{1*}; 牧村 美穂¹; 樋口 明良¹; 渡辺 了¹
SEMA, Fumie^{1*}; MAKIMURA, Miho¹; HIGUCHI, Akiyoshi¹; WATANABE, Tohru¹

¹ 富山大学地球科学科

¹ Department of Earth Sciences, University of Toyama

Pore-fluid pressure in seismogenic zones can play a key role in the occurrence of an earthquake (e.g., Sibson, 2009). Its evaluation via geophysical observation can lead to a good understanding of seismic activities. It is critical to understand how pore-fluid pressure affects seismic velocity and electrical conductivity. We have studied the influence of pore-fluid pressure on elastic wave velocity and electrical conductivity of water-saturated rocks.

Measurements have been made using a 200 MPa hydrostatic pressure vessel, in which confining and pore-fluid pressures can be separately controlled. An aqueous pore-fluid is electrically insulated from the metal work by using a specially designed device (Watanabe and Higuchi, 2013). Elastic wave velocity was measured with the pulse transmission technique (PZT transducers, $f=2$ MHz), and electrical conductivity the four-electrode method (Ag-AgCl electrodes, $f=100$ mHz-100 kHz) to minimize the influence of polarization on electrodes.

Berea sandstone (OH, USA) was used for its high porosity (19.1%) and permeability ($\sim 10^{-13}$ m²). It is mainly composed of subangular quartz grains. Microstructural examinations show clay minerals (e.g., kaolinite) and carbonates (e.g., calcite) fill many gaps between quartz grains. A small amount of feldspar grains are also present. The grain size is 100-200 micrometers. Cylindrical samples have dimensions of 25 mm in diameter and 30 mm in length. Their axes are perpendicular to sedimentation bed. Elastic wave velocity is slightly higher in the direction perpendicular to the axis than in that parallel to the axis.

Confining and pore-fluid pressures work in opposite ways. Increasing confining pressure closes pores, while increasing pore-fluid pressure opens them. For a given pore-fluid pressure, both compressional and shear velocities increase with increasing confining pressure, while electrical conductivity decreases. When confining pressure is fixed, velocity decreases with increasing pore-fluid pressure while conductivity increases. The closure and opening of pores can explain observed changes of velocity and conductivity.

Effective confining pressure is defined by the difference between confining and pore-fluid pressures. Velocity increases with increasing effective confining pressure, while conductivity decreases. However, neither velocity nor conductivity is unique function of the effective confining pressure. For a given effective confining pressure, conductivity significantly increases with increasing confining pressure. Velocity also increases with increasing confining pressure, though it is not so significant. Increasing pore-fluid pressure can compress clay minerals to increase pore space. This might explain observed conductivity change.

キーワード: 間隙流体圧, 地震波速度, 電気伝導度, 地殻流体

Keywords: pore-fluid pressure, seismic velocity, electrical conductivity, geofluid

電気伝導度測定による岩塩中の粒界水の研究 A study on grain boundary brine in halite rocks using electrical conductivity measurements

渡辺 了^{1*}; 北野 元基¹
WATANABE, Tohru^{1*}; KITANO, Motoki¹

¹ 富山大学大学院理工学研究部

¹ Graduate school of science and engineering, University of Toyama

Intercrystalline fluid can significantly affect rheological and transport properties of rocks. Its influences are strongly dependent on the style of distribution. When a fluid fills grain boundaries in a rock, it will significantly reduce the strength of the rock. The fluid distribution is mainly controlled by the dihedral angle between solid and fluid phases. The grain boundary wetting is expected only when the dihedral angle is 0°. The dihedral angle of the halite-water system was studied through microstructural analyses of quenched materials (Lewis and Holness, 1996). The dihedral angle is 50~70° at $P < 200$ MPa and $T < 300$ °C. However, deformation experiments (e.g., Watanabe and Peach, 2002) and cryo-SEM observations (e.g., Schenk et al., 2006) on halite rocks have indicated the coexistence of grain boundary brine with a positive dihedral angle. In order to understand the nature of grain boundary brine, we have conducted electrical impedance measurements on synthetic wet halite rocks over a wide range of pressure and temperature.

Wet halite rock samples (9 mm diameter and 6 mm long) are prepared by cold-pressing ($P=140$ MPa, 40 min.) of wet NaCl powder and annealing ($T=180$ °C, $P=180$ MPa, 160 hours). Grains are polygonal and equidimensional with a mean diameter of 50-100 μ m. The porosity is less than 1%. The volume fraction of brine is estimated to be 11.1% by the thermo gravimetric analysis. Microstructural observation shows that most of brine is enclosed inside halite grains. Electrical impedance is measured in the axial direction of a sample by a lock-in-amplifier (SRS, SR830) with a current amplifier (SRS, SR570). The cylindrical surface of a sample is weakly dried and coated with RTV rubber to suppress the contribution of surface conduction. A conventional externally heated, cold-seal vessel (pressure medium: silicone oil) is used to control pressure and temperature.

Electrical conductivity of wet halite rocks is higher than that of NaCl by orders of magnitude even at the conditions of the dihedral angle larger than 60 degrees. The conduction through brine dominates the bulk conduction. This is also supported by the quick conductivity change in response to the change in pressure. Brine is interconnected over a whole range of pressure and temperature.

No remarkable change in conductivity is observed around the condition of the dihedral angle of 60 degrees. Although the interconnection of triple-junction tubes might drastically change at the dihedral angle of 60 degrees, its influence on the bulk conductivity is masked by more conductive paths. A triple-junction tube is so stiff that it cannot give observed conductivity changes in response to changes in pressure. The dominant conduction paths are not triple-junction tubes. Grain boundary brine must be the dominant conduction paths.

Electrical conductivity decreases with increasing pressure. Larger change is observed for lower temperatures. A simple model of fluid tube with elliptical cross-section shows that the thickness of a fluid tube decreases by less than 10%. The observed large change in conductivity suggests that the conductivity of brine is strongly dependent on the fluid thickness. When the thickness is comparable to the molecular size, the mobility of ions must be sensitive to the thickness. The observed large change in conductivity might be caused by the decrease in ionic mobility.

キーワード: 岩塩, 粒界, 水, 電気伝導度

Keywords: salt, grain boundary, water, electrical conductivity

室内実験による上総層群シルト岩の最大埋没深度の推定 Estimation of the maximum burial depth of siltstones from the Kazusa Group by laboratory experiments

田村 幸枝¹; 丸茂 春菜²; 三橋 俊介¹; 上原 真一^{1*}

TAMURA, Yukie¹; MARUMO, Haruna²; MITSUHASHI, Shunsuke¹; UEHARA, Shin-ichi^{1*}

¹ 東邦大学理学部, ² 東邦大学大学院理学研究科

¹ Faculty of Science, Toho University, ² Graduate School of Science, Toho University

堆積岩の最大埋没深度を推定することは、例えば堆積盆の隆起量や侵食量の推定等に関係して重要である。堆積岩の最大埋没深度を推定する手法の一つとして、土質実験で一般的に実施される室内圧密実験による手法が提案されている。しかしながら、岩石の場合、続成作用において化学的な粒子間の固着等により、この方法では単純に評価できない可能性がある。従って、実際の堆積盆を用いて、本手法の適用性を評価することは重要である。

本研究では、関東平野の基盤である上総層群のシルト岩について、室内実験により、間隙率の有効圧依存性を測定し、その結果に基づいて岩石の最大埋没深度を推定した。その結果と、各層の層序及び層厚から推定された各岩石試料採取地点間の層厚差と比較し、本地域において、最大埋没深度の求め方として本研究の手法が適しているのかを検証した。

実験に使用するシルト岩は、上総層群の梅ヶ瀬層 (UMG) 及び大田代層 (OTD)、黄和田層 (KWD)、大原層 (OHR)、勝浦層 (KTR) (以上、層準的に上位から下位の順番) 露頭より採取した。その岩石ブロックから直径約 40 mm、高さ約 30 mm の円柱形に加工したものを試料として実験に用いた。間隙率実験は容器内圧縮変形透水試験機を用い、有効圧を 0 MPa から 35 MPa (間隙水圧は 1 MPa) の条件で測定を行った。有効圧を加えた時の試料から出た間隙水の体積を測定し、これを試料の体積で割ることで、間隙率の変化量を求めた。この結果を用いて、まず有効圧と間隙率の関係をグラフにし、グラフの折れ曲がっている点の前後の箇所についてそれぞれ近似曲線を引き、その交点から最大経験有効圧 ($P_{e,B}$) を求めた。そして $P_{e,B}$ の値を、湿潤岩石密度から間隙水密度を引いた値に重力加速度をかけた値で割ることで、最大埋没深度 (D_{max}) を推定した。

UMG、OTD、KTR は、上位の層ほど間隙率が高い関係が見られた。一方、OHR と KWD は他の岩石に比べて間隙率が高く、層序順に並ばなかった。OHR 以外は、各採取地点間の層厚差と $P_{e,B}$ には正の相関が見られた。ただし、層厚差と D_{max} 推定値の関係の傾きが 1 とは異なった (約 0.27)。また、UMG と OTD の値は互いに層序的に逆転した。以上のように、本研究の手法による最大埋没深度の推定値は、層厚差と正の相関は見られたものの、いくつか矛盾した点が見られたことから、その適用性については今後更に検討する必要がある。また、OHR は層序が比較的下位に位置するのにも関わらず、 $P_{e,B}$ は他の岩石に比べ低い値となった。これは大原層中の間隙圧が静水圧分布に対し 5~12 MPa 程度高く、そのため有効圧が低かったことを反映している可能性がある。

キーワード: 間隙率, 最大埋没深度, 最大経験有効圧, 上総層群, 異常間隙水圧, 室内岩石実験

Keywords: porosity, maximum burial depth, maximum effective stress experienced, Kazusa Group, overpressure, laboratory rock experiment

アンチゴライトが安定な温度圧力条件下における蛇紋岩化速度に関する実験的研究 Experimental constraints on the serpentinization rate under the antigorite-stable P-T condition

中谷 貴之^{1*}; 中村 美千彦¹
NAKATANI, Takayuki^{1*}; NAKAMURA, Michihiko¹

¹ 東北大学理学研究科地球惑星物質科学科

¹ Earth and Planet Materials Sci., Tohoku Univ.

Water transport into the Earth's interior can be limited by the rate of serpentinization reaction proceeding at slow spreading ridges and along bending related faults (Iyer et al., 2012). Moreover, the distribution of H₂O in the mantle wedge may be controlled by the extent of progression of the reaction between the slab-derived fluid and the hanging wall mantle, as suggested by theoretical models (Iwamori, 1998). Previous hydration experiments for kinetic studies have been vigorously conducted at relatively low P-T condition (up to ca. 400 °C and 0.3 GPa) where the low T serpentine variety lizardite or chrysotile is stable. In contrast, antigorite is expected to be the dominant serpentine variety under the higher P-T condition corresponding to the deep oceanic lithosphere and the mantle wedge.

In order to constrain the serpentinization rates of peridotite under the antigorite-stable conditions, we conducted piston-cylinder experiments at 580 °C and 1.3 GPa. Four types of starting materials were prepared from the crushed powder of a San Carlos lherzolite xenolith: 1) olivine (Ol), 2) orthopyroxene (Opx) + clinopyroxene (Cpx), 3) Ol + Opx, and 4) Ol + Opx + Cpx + spinel. These systems were abbreviated as OL, OPX+CPX, OL+OPX, and LHZ, respectively. The starting materials were reacted with 15 wt% distilled water for 4-15 days. The formation of serpentine + talc + magnetite was observed in all the systems except for OL. Based on Raman spectroscopy results and crystal shapes, the synthesized serpentine mineral was identified as lizardite with 6.9 wt% Al₂O₃, rather than antigorite. The high Al₂O₃ content in the system possibly stabilized the aluminous lizardite at the experimental temperatures. Low silica activity precluded olivine reaction in the OL system, whereas olivine reacted with the SiO₂ component in orthopyroxene to form lizardite and talc in the other systems. The reaction progress followed an interface-controlled rate law. The growth rate, *G*, was estimated to be 2.31 ± 0.37, 1.23 ± 0.20, and 2.78 ± 0.64 μm/day in the OPX+CPX, OL+OPX, and LHZ systems, respectively. As an example, we applied the hydration rates of peridotites, which were obtained experimentally, to a reactive-transport model for the convecting mantle wedge hydration. In the case of grain-scale pervasive flow, the mass flux ratio of water fixable in the hanging wall peridotites to that supplied from the dehydrating oceanic lithosphere was calculated to be 2.7 × 10⁵ - 1.5 × 10⁸. This indicates that the water is completely fixable in the convecting mantle wedge and carried down to the stability limit of serpentine as soon as it is supplied from the slab. Aqueous fluid may penetrate all the way through the serpentine stable layer and reach the hot center of the mantle wedge only when the fluid migrates via crack-like pathways with a spacing >270-15000 m, which is not consistent with observations of natural serpentinites.

キーワード: 加水反応, 蛇紋石, 流体, 沈み込み帯, マントルウェッジ

Keywords: hydration, serpentine, fluid, subduction zone, mantle wedge

シリケートガラス中の水の拡散における速度論的同位体効果 Diffusive kinetic isotope fractionation of water in silicate glasses

黒田 みなみ^{1*}; 山本 大貴¹; 橘 省吾¹; 中村 美千彦²; 奥村 聡²; 朝木 美帆²; 石橋 充子¹; 坂本 直哉¹; 坂本 尚義¹
KURODA, Minami^{1*}; YAMAMOTO, Daiki¹; TACHIBANA, Shogo¹; NAKAMURA, Michihiko²; OKUMURA, Satoshi²;
ASAKI, Miho²; ISHIBASHI, Atsuko¹; SAKAMOTO, Naoya¹; YURIMOTO, Hisayoshi¹

¹ 北海道大学大学院理学研究院, ² 東北大学理学系大学院地学専攻

¹Department of Natural History Science, Hokkaido University, ²Department of Earth Science, Tohoku University

火道内を上昇するマグマ中で過飽和状態となった揮発性成分は、核形成を経て拡散によって、より大きな気泡へと成長する。これらの過程は揮発性成分の溶解度および拡散係数により支配されているため、メルト中の揮発性成分の挙動を理解することは、噴火メカニズムおよびダイナミクスを知る上で重要となる。

火道内での脱ガス過程は、気泡とメルト中に溶解した水との間で行われる同位体交換反応を通じ、水素同位体比に記録されていると考えられている。天然の岩石に含まれる水素同位体比は含水量と相関があり、含水量が低い程同位体比は小さくなり、その減少率は含水量の減少に伴い大きくなる。この傾向は閉鎖系脱ガスから開放系脱ガスへの推移を反映していると考えられるが、現在考えられている脱ガスモデルには、マグマ中の拡散の効果が考慮されていない。拡散による脱ガスは、マグマの上昇に伴う減圧脱ガスと同程度の影響を、脱ガスプロセス全体に与えている可能性があるため、より詳細な脱ガスモデルを組み立てる際には拡散の影響を考える必要がある。さらに、シリケートメルト中の水の拡散では、 H_2O が HDO に比べ拡散しやすいことが考えられるため、速度論的同位体効果が起きていることが予想される。この影響は天然試料の D/H にも記録されている可能性がある。しかし、シリケートメルト中の水の拡散における水素同位体変化は未だ明らかになっていない。本研究では、水素の拡散による同位体分別係数を決定するために、シリカガラスと合成ライオライトガラスに対し、重水素の濃集させた水試料 ($H/D = 10, 5, 1$) を用いた拡散実験を行った。

実験はシリカガラスおよび合成ライオライトガラスを用い、石英管封入による実験 (850 °C, 50 bar) と、東北大学の水熱装置を用いた実験 (650 °C, 50・1000 bar) の二種類を行った。ガラスサンプルは、イオンマイクロプローブ (北海道大学の Cameca ism-6f) で H, D の濃度プロファイルを測定し、拡散係数の決定を行った。実験によって得られた H_2O , HDO を含む水の拡散係数 (水の濃度で割った値) は、650 °C, 850 °C 共に先行研究 (Davis and Tomozawa, 1995; Berger and Tomozawa, 2003) と矛盾しないことが確かめられている。また、本研究ではシリカガラスについて、拡散に伴う D/H 変化の測定を行った。その結果、D/H が拡散に伴い一度減少し、その後プロファイルに沿って増加することが確認された。D/H が下がる現象は拡散に伴う速度論的同位体効果が影響していることが考えられるが、その後の増加は拡散の同位体効果だけでは説明することができない。この現象は含水量変化に伴う IMF (Instrumental Mass fractionation) の変化によるものだと考えることができるため (Hauri et al., 2006), 今後、水素同位体変化を正確に補正するため、IMF の値を決定することが必要である。

キーワード: 噴火ダイナミクス, ケイ酸塩ガラス, 水, 拡散, 水素同位体, 同位体効果

Keywords: eruption dynamics, silicate glass, water, diffusion, hydrogen isotope, isotopic fractionation

超高精度地質圧力計の開発 Development of high-precision geobarometer

高畑 幸平^{1*}; 鳥本 淳司²; 山本 順司²
TAKAHATA, Kohei^{1*}; TORIMOTO, Junji²; YAMAMOTO, Junji²

¹ 北海道大学大学院理学院自然史科学専攻地球惑星システム科学講座, ² 北海道大学総合博物館
¹Earth and Planetary System Science, Hokkaido University, ²Hokkaido University Museum

マントル捕獲岩は、我々が手にする事が出来るマントル物質の一つである。マントル捕獲岩は由来深度が分からないため、この岩石を用いて地球深部の定量的な議論をするためには、地質圧力計を適用して由来深度を復元することが重要である。

マントル捕獲岩にはスピネル-レルゾライトと呼ばれる、かんらん石、斜方輝石、単斜輝石、スピネルからなる種類の岩石がある。このスピネルを含む捕獲岩の由来深度は定性的におよそ 25 — 90 km といわれており、最上部マントルから来た岩石である事が推定される。よって、この岩石の由来深度が精密に計りとる事が出来れば、マントル最上部で起きている事象を定量的に議論する事が出来る。

このマントル捕獲岩に従来から適用されてきた地質圧力計として、ざくろ石-斜方輝石圧力計とかんらん石-単斜輝石圧力計がある。しかし、前者はざくろ石の入っていない岩石には適用出来ず、後者は分析誤差や圧力計が持つ温度依存性の影響で圧力誤差が大きすぎる為、定量的な議論が出来ない。つまり、スピネル-レルゾライトを使って最上部マントルの議論をする為には、新たに高精度な地質圧力計を開発する必要がある。

そこで、本研究では CO₂ 流体包有物の残存圧力を圧力指標とした地質圧力計に必要な、ラマン分光法を用いた高精度な密度測定を実現する為のラマン分光分析装置の開発と、その精度の決定を行った。開発に際して、分光器の焦点距離を伸ばし、波数分解能を向上させた新たなラマン分光分析装置を導入した。

サンプルは、ラマンスペクトルの強度が出やすい石英中の CO₂ 流体包有物を使用した。また、このサンプルの包有物中に CO₂ 以外の不純物が含まれるか加熱ラマン分光法で確認した。

測定の結果、新しい装置による密度測定誤差は、 $\pm 0.0025 \text{ g/cm}^3$ (1 σ) となった。この密度誤差は、圧力誤差にする際の輝石温度計の誤差に比べて非常に小さい為、この地質圧力計の誤差は、すなわち、輝石温度計に起因する誤差のみとなる。よって、この圧力計の深さ誤差は、大陸地殻のモホ面深度付近 (30 km) で地質温度が $1000 \pm 30^\circ \text{C}$ と見積もられた場合で、 $\pm 900 \text{ m}$ となる。

この精度があれば、最上部マントルで起きている様々な事象を地球物理的な手法よりも高解像度に議論する事が出来る。

キーワード: 流体包有物, 二酸化炭素, ラマン分光法, マントル捕獲岩, 地質圧力計

Keywords: fluid inclusion, carbon dioxide, Raman spectroscopy, mantle xenolith, geobarometer

高精度ホウ素同位体比迅速分析法の地下水・火山岩への応用 Applications of rapid and precise $^{11}\text{B}/^{10}\text{B}$ isotopic analysis to water and rock samples

谷水 雅治^{1*}; 永石 一弥²; 石川 剛志¹
TANIMIZU, Masaharu^{1*}; NAGAISHI, Kazuya²; ISHIKAWA, Tsuyoshi¹

¹ 海洋研究開発機構高知コア研究所, ² マリンワークジャパン
¹Kochi Institute, JAMSTEC, ²Marine Works Japan Ltd.

Boron isotope ratio is a powerful tracer in the fields of geochemistry, biochemistry, and environmental chemistry. Boron isotope ratios are determined by TIMS or MC-ICP-MS with precisions of better than 0.1 % RSD, but a large inter-lab discrepancy of 0.6 % is still observed for actual carbonate samples (Foster, 2008). Here, we are trying to determine B isotope ratio by MC-ICP-MS with a simple and common analytical techniques using a quartz sample introduction system with a PFA nebulizer, and compared to recently developed precise B isotope ratio analysis techniques by TIMS in positive ion detection mode determined as Cs₂BO₂⁺ ions with sample amount of <100 ng (Ishikawa and Nagaishi, 2011) and by MC-ICP-MS (Foster, 2008, Louvat et al., 2011).

In this year, our developed B analytical method above for carbonate and water samples are applied to rock samples. Resultant analytical reproducibility (twice standard deviation) was +/-0.04 % with a consumption of 50 ng B for several geochemical reference rocks issued from GSJ. Their relative differences from the standard were consistent with those determined by the positive TIMS within analytical uncertainty. Current potential B isotopic analysis by MC-ICP-MS will be discussed.

スラブとともに沈み込む水の移動と全マントル対流への動的効果 Water migration with a subducting slab and the dynamic effects on whole mantle convection

金子 岳郎^{1*}; 中久喜 伴益¹; 岩森 光²
KANEKO, Takeo^{1*}; NAKAKUKI, Tomoeiki¹; IWAMORI, Hikaru²

¹ 広島大学大学院理学研究科地球惑星システム学専攻, ² 海洋研究 開発機構・地球内部物質循環研究分野
¹Dept. Earth and Planetary Systems Science, Hiroshima Univ, ²Geochemical Evolution Research Program, JAMSTEC

Existence of liquid water is a characteristic of the earth. The water of interior of the Earths involved with the subducting plate reduces density and viscosity of the crustal and mantle rocks. These effects are essential to emerge the solid Earth activity such as, plate tectonics and island arc volcanism. Although the most of subducted water circulates through upper mantle, there is a possibility that portion of the water penetrates into lower mantle. Where does the water migrate? How much does the water affect mantle dynamics through the rock rheology and property? We performed numerical mantle convection simulation to investigate the water cycle and dynamic effects on the whole mantle convection.

In this study, we use the numerical model based on the model (Tagawa et al., 2007; Nakakuki et al., 2010) including the subducting oceanic plate driven dynamically. This model includes migration of water with the plate motion. We consider influences of reducing density and viscosity due to the water on the mantle flow (Karato and Jung, 2003). The maximum water content in the upper mantle is determined using phase relations of the basalt and the peridotite (Iwamori, 2004; 2007). We use various values of the maximum water content of rocks in the lower mantle, because it has been not clearly defined. We also treated the following physical properties as varying parameters: friction coefficient at the plate boundary, amount of the water injection at the trench, density-water dependence coefficient, and maximum water content in the lower mantle. Addition to we calculated dislocation creep by non-newtonian fluid or newtonian fluid.

A part of subducted water associate with the subducting oceanic plate is absorbed into peridotitic rocks and transported to about 150 km deep mantle. After that, dehydration with the serpentine decomposition occurs, and transported to deeper mantle by hot nominally anhydrous minerals (NAMs). The amount of dehydration at the 660 km phase boundary depends on the maximum water content of lower mantle, when the slab penetrates into lower mantle. The ejected water forms thin and high-water-content layer over the 660 km phase transition. As a result, the buoyancy of this layer induces instability, so that hydrated plumes are generated. We propose that this mechanism is important for the water cycle in the upper mantle. On the other hand, considerable portion of the water is transported into lower mantle with subducting slab, although notable water capacity of the lower mantle much smaller than that of the upper mantle, and reach core-mantle boundary. We have not yet observed notable water influence on mantle convection at lowermost mantle because of the small water concentration. Also, the hydrated materials do not rise to surface with hot plumes generated at the core-mantle boundary.

Keywords: mantle convection, plume, transition zone, water transport